

DYNAMIC BEHAVIOR OF ROTOR SURROUNDED BY OUTER CASTING WITH SMALL ANNULAR CLEARANCE

Sagheer Ahmad¹, M.K.K.Ghauri²

Abstract

Vibration response of a rotor surrounded by an outer casing is investigated. For the analysis, a six-degree-of-freedom dynamic model of a shaft and disk is established using Lagrangian equations. While deriving the differential equations of motion, gyroscopic effect was taken into account and the solution of equations and response was obtained in MATLAB. Results demonstrate that rotor-stator rubbing may occur in a variety of forms and circumstances. It is shown that the inclusion of gyroscopic effect in the vibration model is useful in revealing the nature of vibration response.

Keywords Rotor, contact, Vibrations, Lagrangian, Gyroscopic effect

Introduction

For high thermal efficiency of turbo-machinery, the clearance between the rotating and stationary elements is kept very small. During malfunctioning, the stationary and rotating elements come in contact with each other resulting in partial or full rub. Rotor-casing rub has been the area of interest of many researchers. Much research has been carried out to understand the rotor/casing motion and to find ways to prevent serious damages resulting from the unstable rubbing vibration. Bazen [1] discussed the effects of friction and alignment on vibration response of interacting surfaces. The mathematical model presented by Currami [2] relates the rotor stiffness to parametric instability. Special attention was given by Choy et al [3] to determine the effects of casing stiffness, friction coefficient, mass imbalance and damping characteristics on the response. Large rub forces were experienced by increasing the casing stiffness and imbalance of the rotor. But damping tends to retard the initiation of backward whirl. It was proved by Zhang [4] that dry friction is the main cause of whirl during rubbing due to which instability occurs. Choy [5] observed the vibration response for the cases of blade loss and varying bearing clearances. Crandall [6] and Childs [7] investigated that large clearance between rotor and casing is needed for the occurrence of dry friction whirl and whip. Wu and Flowers [8] concluded that severity of rub depends on lubrication of interacting surfaces and acceleration of rotor. Goldman and Muszynska [9] showed that increase in temperature results in oscillation of rotor. Chu and Lu [10] concluded that rubbing results in increased stiffness of interacting surfaces. Feng et al [11] demonstrated that forward whirling of rotor results in the absence of friction and full rubbing behaves as backward whirling due to friction. It was demonstrated by Karpenko et al [12] that increased intensity of out-of-balance generates full annular rub. Qin et al [13] showed that chaotic motion is due to increase in the external damping of rotor-casing system. Jiang et al [14] studied the effects of different system parameters such as stiffness, damping and mass imbalance on the vibration behavior. Jiang [15, 16] included in his vibration model the effect of dry friction and predicted the self-excited vibrations of the rotor with the amplitude fluctuating around the critical value of the deflection. It is interesting to note from the above described survey that the details of early warning response characteristics prior to interaction of rotating and stationary elements are missing in the published literature.

Effect of gravity on rotor in the analyses. In the present study, rotor considered is vertical and effect of gravity has been considered. Gyroscopic effect has also been included, which, to the authors' knowledge has not been taken into account in a vertical rotor system in the past conducted researches. In this paper, the dynamic response of a vertical flexible rotor before its interaction with the outer casing has been presented. The aim is to contribute to the development of efficient method for understanding the

^{1&2}Department of Mechanical Engineering, University of Engineering & Technology, Taxila, Pakistan, engr_sagheer@hotmail.com

behavior of a rotor system under the influence of certain system's parameters which have been frequently used by the past researchers.

Rotor-Stator Model

The test rig (Figure-1) consisted of a flexible shaft vertically clamped, coupled with driving motor at the upper end through a flexible coupling and carrying a disk at the lower end. The shaft is rigidly connected to the foundation (outer casing) through a set of horizontal springs and viscous dampers at a distance of three quarter of shaft's length from the upper end. A suitable gap of 10 mm is kept between disk and the outer casing. Eddy current type displacement transducers and accelerometers (ENDEVCO 100 mv/g) were used for obtaining the signals from the rotor/casing system. For data acquisition and analysis, a Fast Fourier Transform (FFT) analyzer made by Bruel & Kajeer was arranged from Directorate of Nuclear Power Engineering Reactor, Pakistan Atomic Energy Commission, and Islamabad, Pakistan.

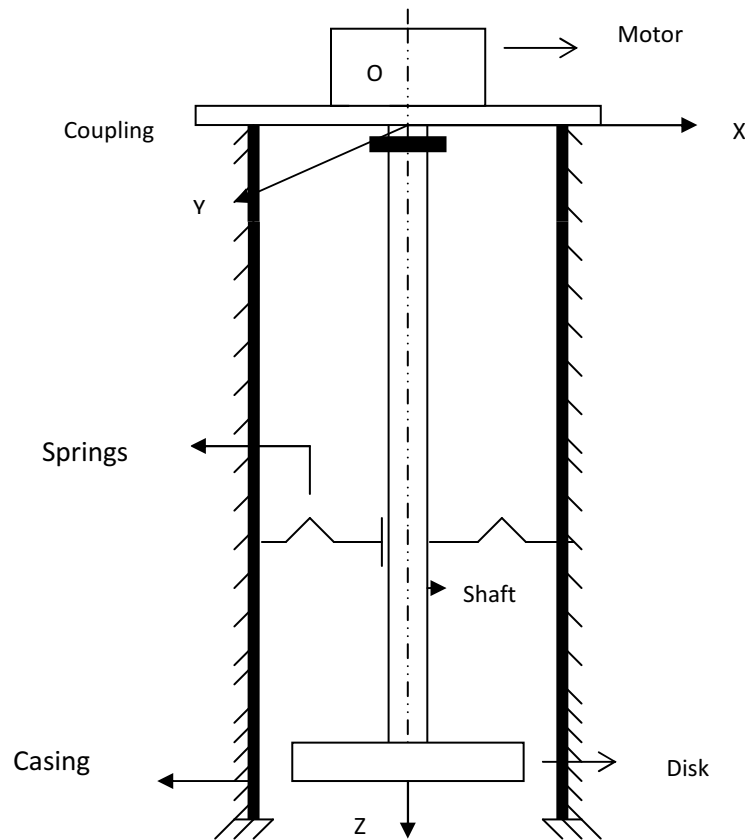


Figure 1. Physical model of the system

The dynamic motion of the system is described by six degrees-of-freedom as θ_x , θ_y , X_{s1} , X_{s2} , Y_{s1} and Y_{s2} as shown in (Figure-2). In the rigid pendulum like mode, the degrees-of-freedom are θ_x and θ_y . Whereas X_{s1} , X_{s2} and Y_{s1} , Y_{s2} represent the degrees-of-freedom in the 1st shaft flexing mode and in the 2nd shaft

flexing mode respectively. The physical characteristics of the model and complete nomenclature are given in the appendix.

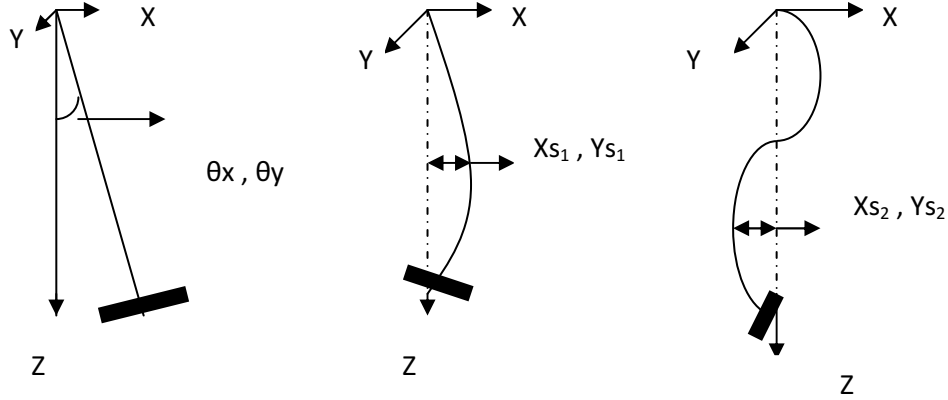


Figure 2. Degrees-of-freedom of the model and gyroscopic effect

Mathematical Model

In developing the rotordynamic model, radial symmetry is assumed. i.e., $K_x = K_y$ and $C_x = C_y$. Springs and Viscous dampers are assumed to be linear and all the deflections in the considered modes of vibrations are assumed to be very small. Gyroscopic effect is taken into account by considering the turning motion of the disc about the X- and Y-axes during its rotation about the Z-axis (Figure-2) resulting from gyroscopic couple. Three modes of vibrations namely, the rigid pendulum like mode, 1st shaft flexing mode and the 2nd shaft flexing mode are considered. In the context of this paper, it is impractical to write all the steps involved in the derivation of differential equations of motion. However, for the purpose of clarity, the main steps are discussed here.

The motion of the system is described in the reference frame OXYZ (Figure-1) using six generalized coordinates. Lagrange's equations are used for obtaining differential equations of motion.

$$\frac{d}{dt} \left(\frac{\partial T}{\partial \dot{q}} \right) - \frac{\partial T}{\partial q} + \frac{\partial U}{\partial q} + \frac{\partial D}{\partial \dot{q}} = Q \quad (1)$$

where $\{q\}^T = [\theta_y, X_{s1}, X_{s2}, \theta_x, Y_{s1}, Y_{s2}]$ is the vector of generalized coordinates.

T, U and D represent total kinetic energy, total strain energy and energy dissipation function of the system respectively. The equations are written in matrix form with **M**, **C** and **K** as mass, damping and stiffness matrices. The resulting linearized equations of motion are:

$$\mathbf{M}\ddot{q} + \mathbf{C}\dot{q} + \mathbf{K}q = Q \quad (2)$$

where $\mathbf{C} = \mathbf{C}^D + \mathbf{C}^G$

\mathbf{C}^D = damping matrix due to external viscous damping

\mathbf{C}^G = damping matrix due to gyroscopic effect.

and $\{Q\}^T = [1, 0, 0, -i, 0, 0].me\omega^2 e^{i\omega t}$

is the vector of forces due to mass imbalance 'me' in the disc.
The mass matrix **M** is given as

$$\begin{bmatrix} \left(\frac{m_s l^2}{3} + m_d l^2 \right) & -\frac{m_s l}{\pi} + \frac{\pi m_d r_d^2}{2l} & \frac{m_s l}{2\pi} - \frac{\pi m_d r_d^2}{l} & 0 & 0 & 0 \\ -\frac{m_s l}{\pi} + \frac{\pi m_d r_d^2}{2l} & \left(\frac{m_s}{2} + \frac{\pi^2 m_s r^2}{2l^2} \right) & -\frac{\pi^2 m_d r_d^2}{l^2} & 0 & 0 & 0 \\ \frac{m_s l}{2\pi} - \frac{\pi m_d r_d^2}{l} & -\frac{\pi^2 m_d r_d^2}{l^2} & \left(\frac{m_s}{2} + \frac{2\pi^2 m_s r^2}{l^2} \right) & 0 & 0 & 0 \\ 0 & 0 & 0 & \left(\frac{m_s l^2}{3} + m_d l^2 \right) & \frac{m_s l}{\pi} - \frac{\pi m_d r_d^2}{2l} & -\frac{m_s l}{2\pi} + \frac{\pi m_d r_d^2}{l} \\ 0 & 0 & 0 & \frac{m_s l}{\pi} - \frac{\pi m_d r_d^2}{2l} & \left(\frac{m_s}{2} + \frac{\pi^2 m_s r^2}{2l^2} \right) & -\frac{\pi^2 m_d r_d^2}{l^2} \\ 0 & 0 & 0 & -\frac{m_s l}{2\pi} + \frac{\pi m_d r_d^2}{l} & -\frac{\pi^2 m_d r_d^2}{l^2} & \left(\frac{m_s}{2} + \frac{2\pi^2 m_s r^2}{l^2} \right) \end{bmatrix}$$

The damping matrix **C** is

$$\begin{bmatrix} \frac{9}{16} C_x l^2 & -0.53 C_x l & -0.75 C_x l & -(m_s r^2 \omega + m_d r_d^2 \omega) & 0 & 0 \\ -0.53 C_x l & 0.5 C_x & 0.707 C_x & 0 & \frac{\pi^2 m_s r^2 \omega}{2l^2} & 0 \\ -0.75 C_x l & 0.707 C_x & C_x & 0 & 0 & 2 \frac{\pi^2 m_s r^2 \omega}{l^2} \\ (m_d r_d^2 \omega + m_s r^2 \omega) & 0 & 0 & \frac{9}{16} C_y l^2 & 0.53 C_y l & 0.75 C_y l \\ 0 & -\frac{\pi^2 m_s r^2 \omega}{2l^2} & 0 & 0.53 C_y l & 0.5 C_y & 0.707 C_y \\ 0 & 0 & -2 \frac{\pi^2 m_s r^2 \omega}{l^2} & 0.75 C_y l & 0.707 C_y & C_y \end{bmatrix}$$

and the corresponding stiffness matrix \mathbf{K} is

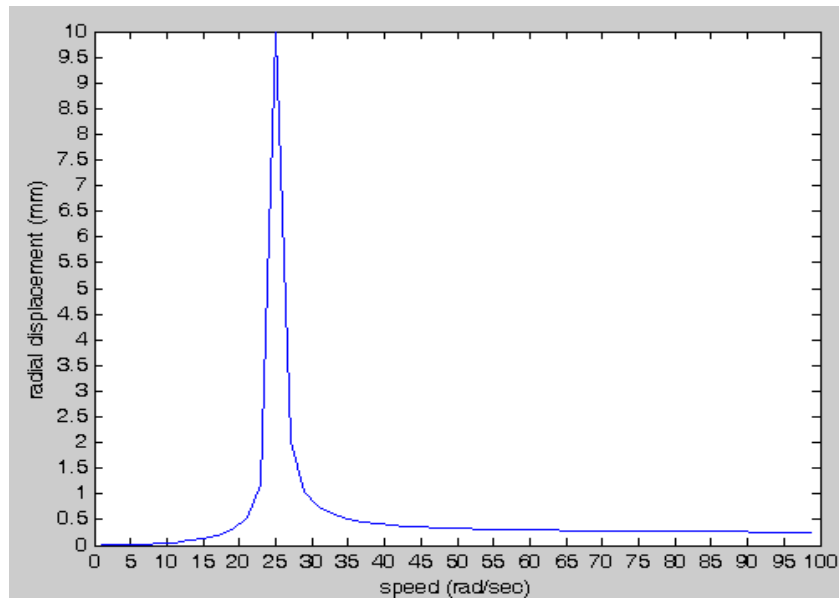


Figure 3. System response with gyroscopic effect

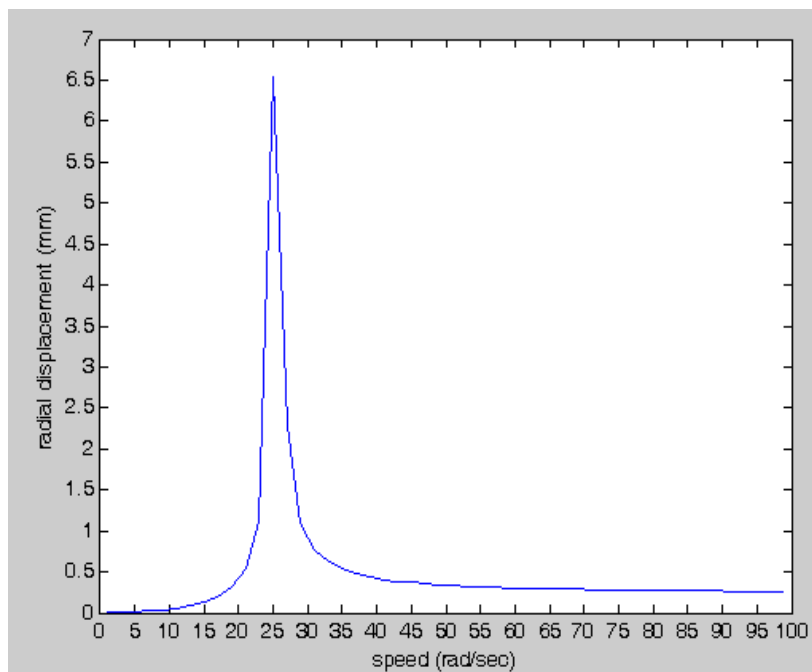
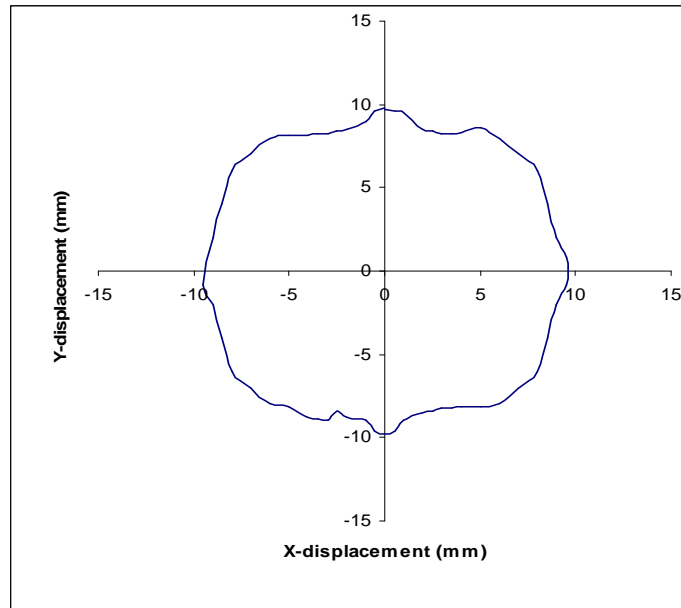
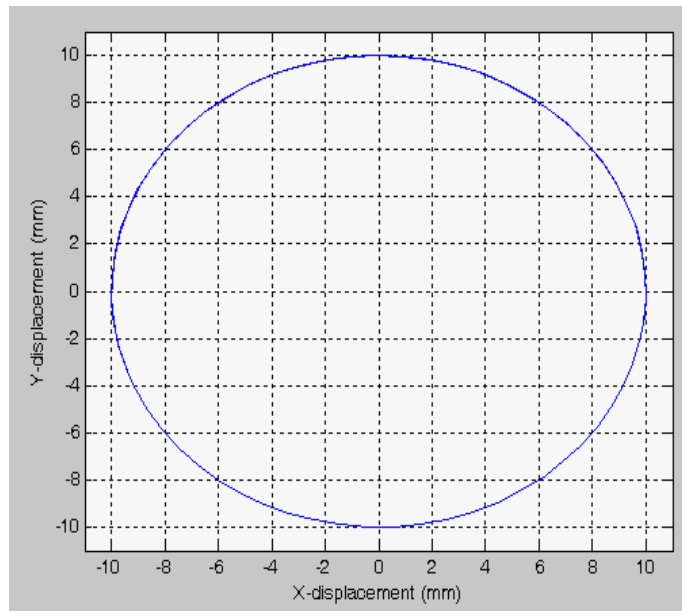


Figure 4. System response without gyroscopic effect

The corresponding motion orbits are shown in Figures- 5 and 6. It can be concluded that it is the gyroscopic effect which ensures the full rubbing of the rotor-disk system with the outer casing. Hence the effects of some other parameters on system's response were studied by incorporating C^g in the mathematical model.



(a) Experimental



(b) Computer predicted

Figure 5. Motion orbit with gyroscopic effect

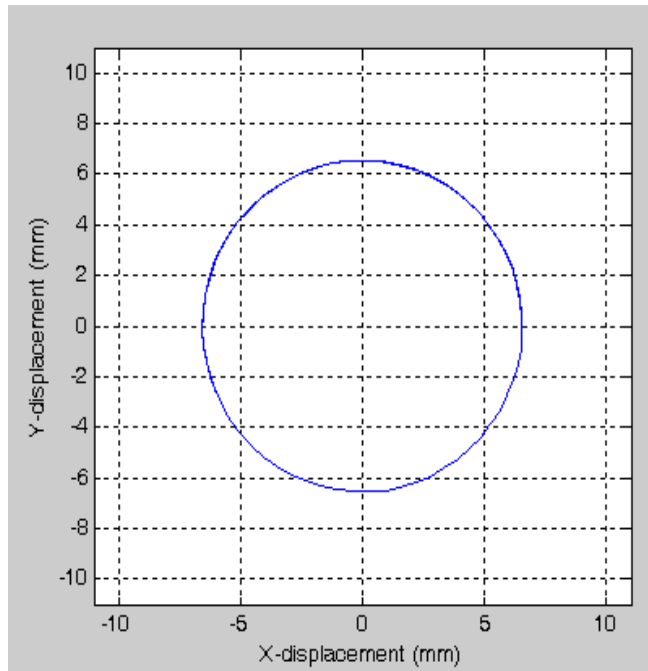
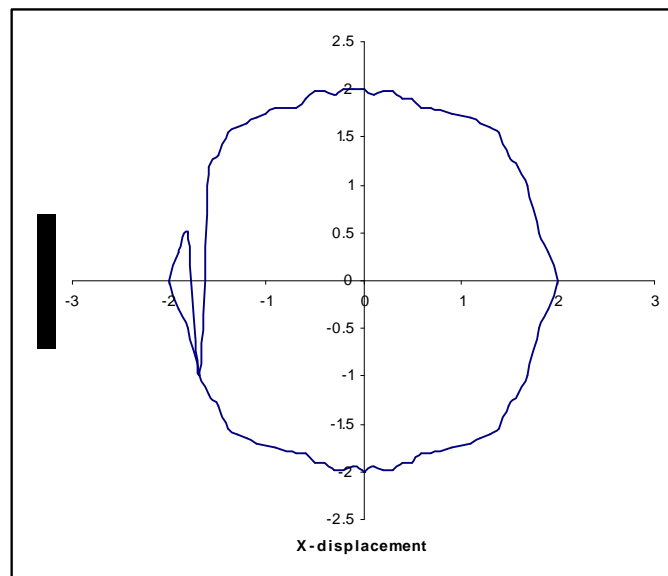
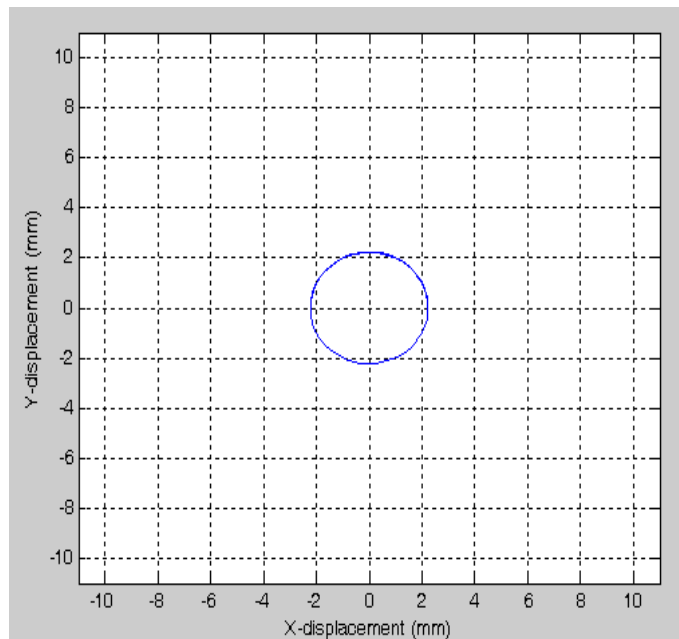


Figure 6. Computer predicted Motion orbit without gyroscopic effect

Rotating speed is an important parameter affecting the vibration response of rotor/casing system. It is noted from Figures- 7 and 8 that full rubbing is not possible at $\omega = 24$ rad/sec and $\omega = 30$ rad/sec.

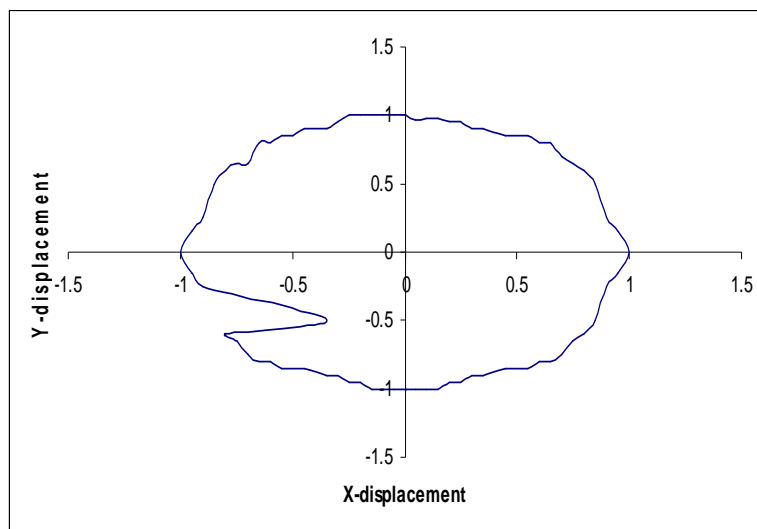


(a) Experimental

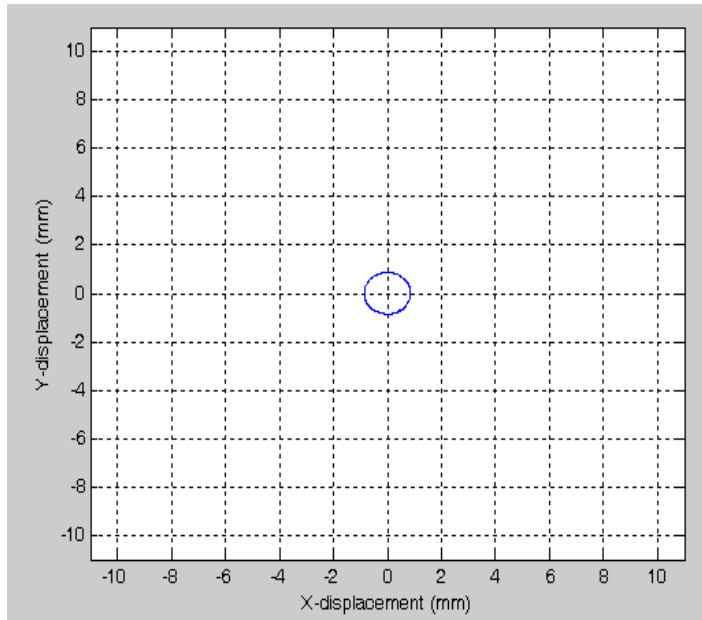


(b) Computer predicted

Figure 7. Steady state response at $\omega = 24$ rad/sec

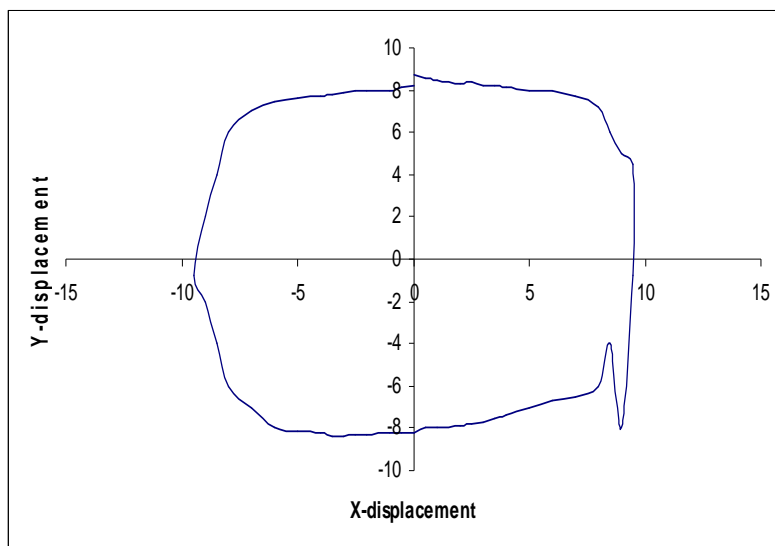


(a) Experimental

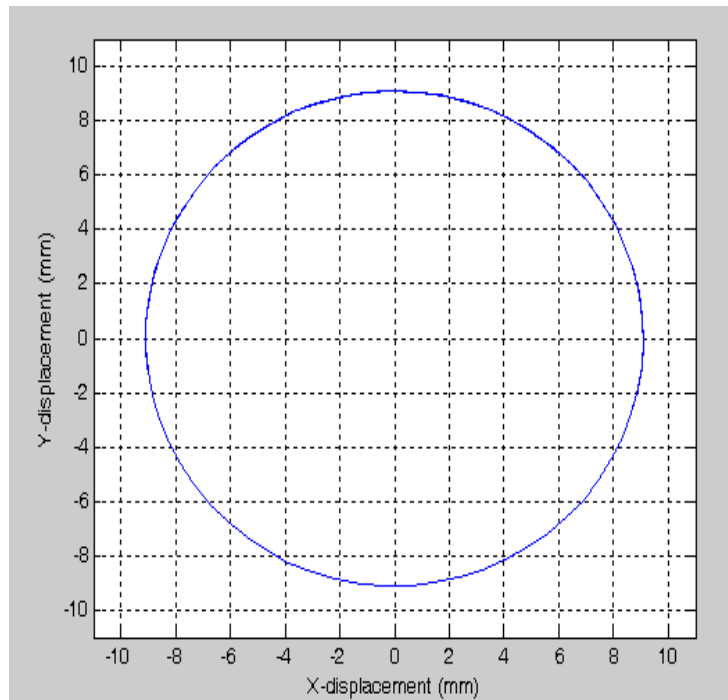


(b) Computer predicted
Figure 8. Steady state response at $\omega = 30$ rad/sec

With the increase in speed from zero to a value equal to 1st natural frequency of the system, the rotor starts rubbing against the casing. With further increase in speed, the contact breaks. With the introduction of damping, the amplitude of vibration may be suppressed as shown in Figures-9 and 10. i.e., as an example, at $\omega = 25.64$ rad/sec and $C_x = C_y = 20$ N-sec/m, full rubbing is not possible.



(a) Experimental



(b) Computer predicted

Figure 9. Steady state response at $\omega = 25.64$ rad/sec , $C = 20$ N-sec/m

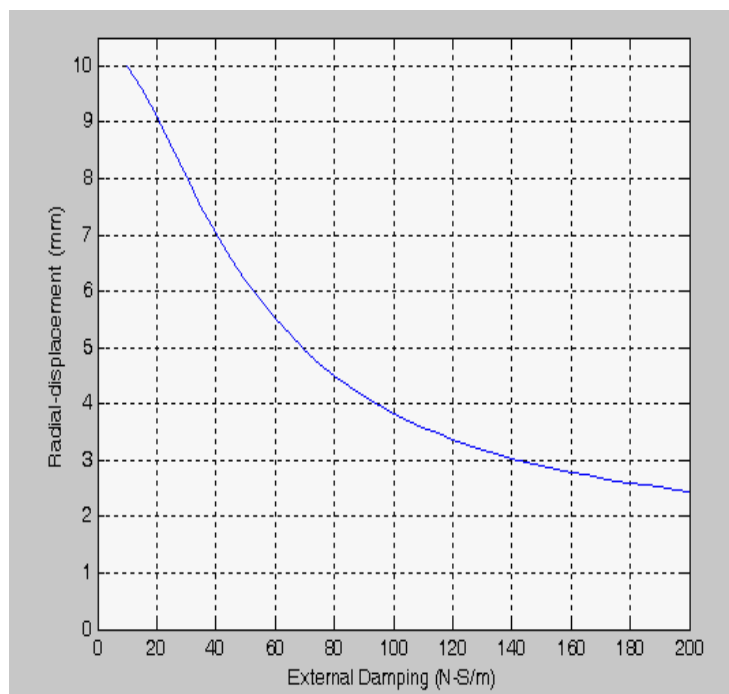
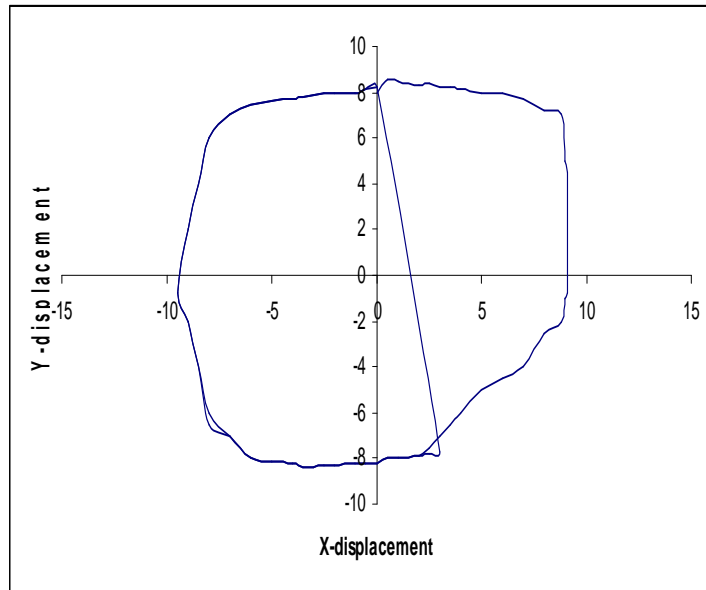
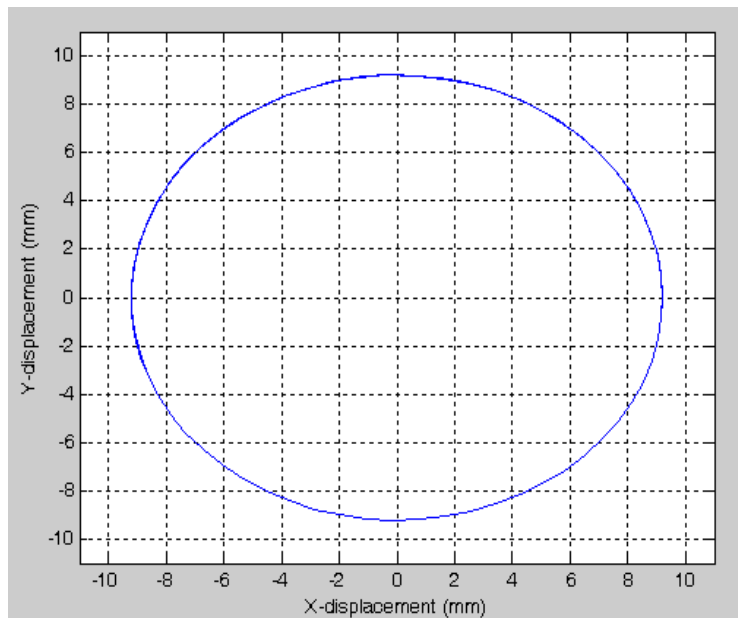


Figure 10. Effect of External Damping

To investigate the effect of stiffness on the dynamic response, the response was plotted for various stiffness values at constant angular speed in Figure-12, keeping all the other parameters fixed. As an example in Figure-11, rubbing is not observed for stiffness equal to 5100 N/m. By increasing the stiffness parameter, rubbing is avoided.



(a) Experimental



(b) Computer predicted

Figure 11. Steady state response for $K_x = K_y = 5100$ N/m

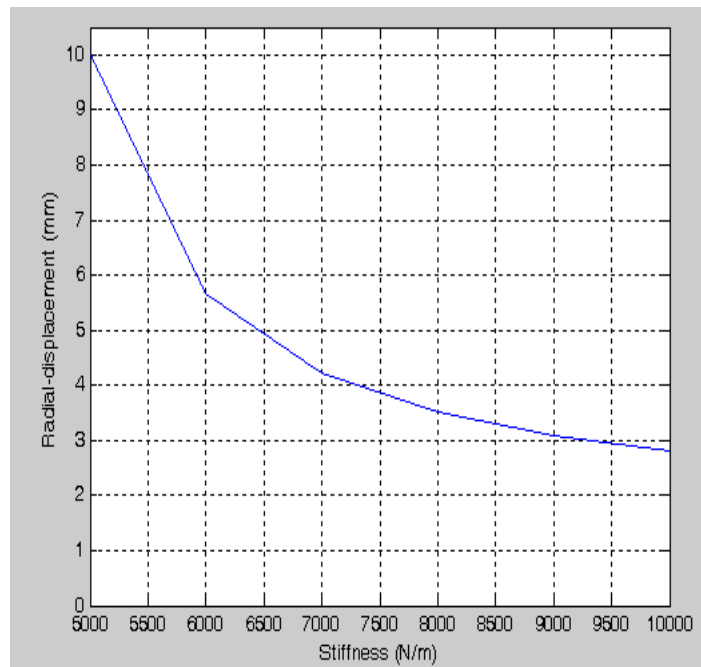
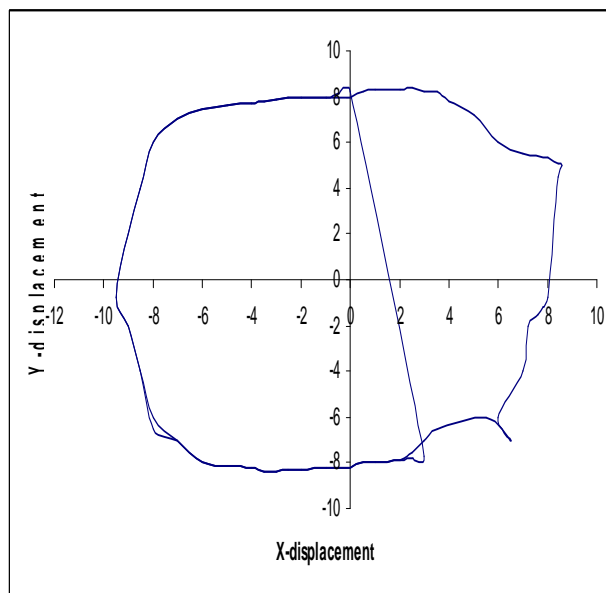
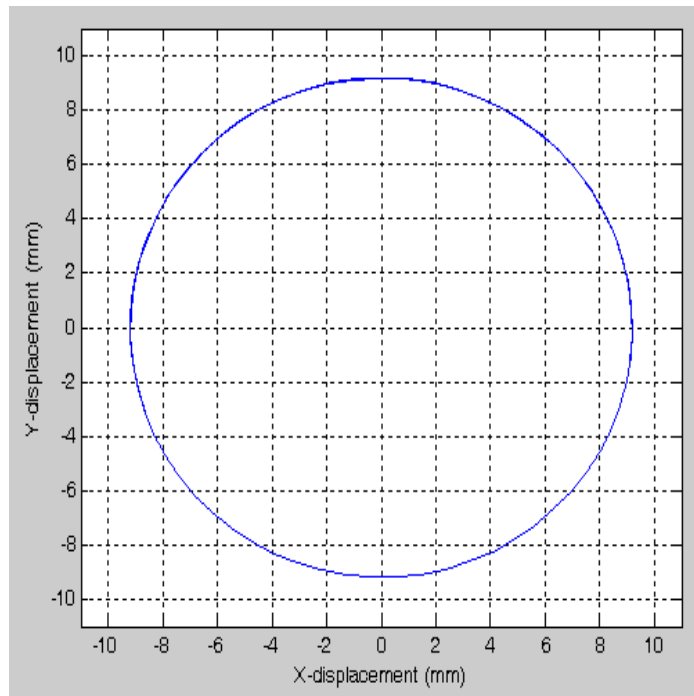


Figure 12. Effect of stiffness

Rotor imbalance is another important parameter affecting the dynamic behavior of the system. In the case of 80 gm-mm un-balance, the rotor did not make contact with the casing at rotating speed of 25.64 rad/sec as given in Figure-13. At the same rotating speed, Figure-14 shows the motion orbit of the rotor with rubbing in the case of imbalance equal to 87 gm-mm. It has been observed that this value of imbalance causes the largest response keeping the rotating speed constant, i.e., for causing rubbing between rotor and casing, the amplitude of imbalance must exceed a certain value known as the critical rubbing excitation.

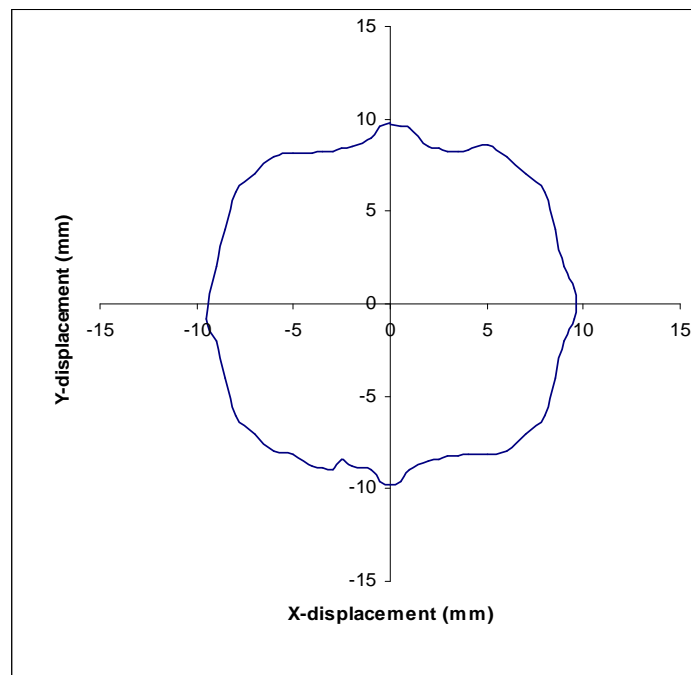


(a) Experimental

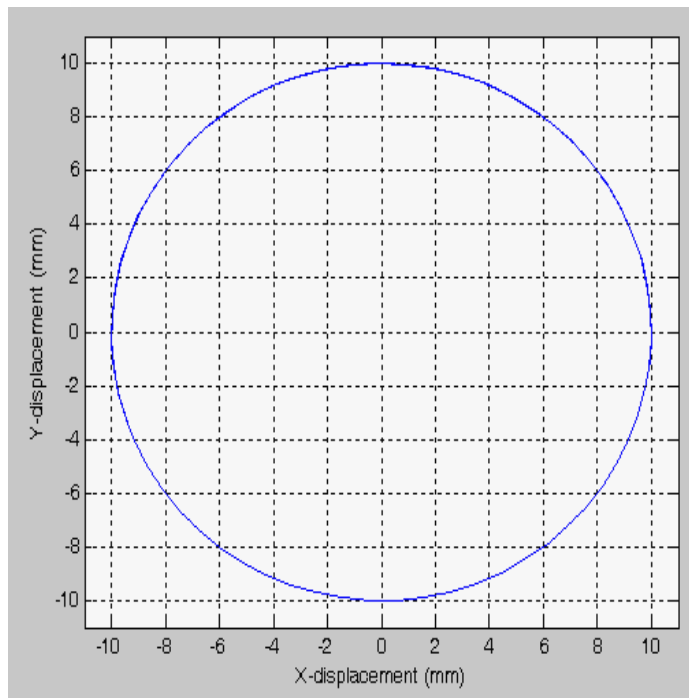


(b) Computer predicted

Figure 13. Steady state response at $m_e = 80$ gm-mm



(a) Experimental



(b) Computer predicted

Figure 14. Steady state response at $m_e = 87$ gm-mm

Conclusion

The dynamic vibration response of a flexible rotor/casing system before its interaction with the outer casing is obtained taking into account the gyroscopic effect. The simulation is carried out in MATLAB under variations in system's parameters. The conclusions are summarized as follows:

- The inclusion of gyroscopic effect in the vibration model is useful in revealing the nature of vibration response.
- The results demonstrate the dependence of the motion on system's parameters like imbalance, speed of rotation, stiffness, damping etc.
- It is shown that by selecting the optimal system's parameters, the harmful heavy rubbing between the rotating and stationary parts can be avoided.

References

- [1] Bazan, E., Bielak J., and Griffin, J.H., 1986 "An Efficient Method for Predicting the Vibratory Response of Linear Structures with Friction Interfaces", Journal of Engineering for Gas Turbines and Power, Volume 94, pp 117-125.
- [2] Currami, A., Pizzigoni, B. and Yania, A.1986, "On the Rubbing Phenomenon in TurboMachinery", Proceedings of the Fourth IFToMM International Conference on Rotordynamics, Tokyo,Japan 1986.pp.481-486.
- [3] Choy, F.K and Padovan, J,1987, " Non-Linear Transient Analysis of Rotor-Casing Rub Events", J ournal of Sounds and Vibrations, 113(3),pp 529-545.
- [4] Zhang, W.,1988 "Dynamic Instability of Multi-Degree-of-Freedom Flexible Rotor System due to Full Annular Rub". Institute of Mechanical Engineering , C 252/88. pp 305-30,.
- [5] Choy, F.K., Padovan,J., Batur,C., 1989 "Rub Interactions of Flexible Casing Rotor System".,